NRC Research Press

ARTICLE

Active transform faults in the Gulf of Guinea: insights from geophysical data and implications for seismic hazard assessment[1]

Mustapha Meghraoui, Paulina Amponsah, Paul Bernard, and Bekoa Ateba

Abstract: The seismotectonics of Western Africa show the occurrence of major earthquakes (e.g., 1636 southwestern Ghana, 1855 offshore Monrovia, 1939 offshore Accra, and 1983 Gaoual-Guinea) and prominent offshore transform faults. However, there is no analysis that links the continental active tectonics with the oceanic fault zones of the Gulf of Guinea. We study the active tectonics by firstly mapping the main transform faults using a combination of bathymetric, gravimetric, and magnetic data. The data analysis associates regional seismicity (historical and instrumental) with focal mechanisms as extracted from the recently published seismotectonic map of Africa. We identify active transform faults, the Chain (CFZ), Romanche (RFZ), Saint Paul (SPFZ), and Arkhangelskiy (AFZ) fault zones. We also calculate strain rates on these faults from Late Cretaceous (~85 Ma) to present time using paleomagnetic data and infer slip rates from the seismic moment data. The strain rates show a first stable trend around 2 cm/year and then accelerate to 4 cm/year in the last 10 million years. The comparison of Late Quaternary strain rates with geodetic strain rates shows an accumulation of seismic energy that could lead to the initiation of an Mw 7–7.5 earthquakes on the Saint Paul transform fault. Our seismotectonic analysis clearly links oceanic and continental tectonics, with about a 20°–30° anticlockwise fault trend rotation for CFZ, RFZ, and SPFZ. The potential for the occurrence of large earthquakes in the Gulf of Guinea should be taken into account for a realistic regional seismic and tsunami hazard of the Gulf of Guinea.

Key words: West Africa, Gulf of Guinea, transform faults, seismic hazard assessment.

Résumé : La sismotectonique de l'Afrique de l'Ouest comprend de grands séismes (p. ex., ceux de 1636 dans le sud-ouest du Ghana, 1855 au large de Monrovia, 1939 au large d'Accra et 1983 à Gaoual en Guinée) et d'importantes failles transformantes océaniques. Il n'existe toutefois aucune analyse reliant la tectonique continentale active aux zones de fractures océaniques dans le golfe de Guinée. Nous étudions la tectonique active en cartographiant d'abord les principales failles transformantes à l'aide des données bathymétriques, gravimétriques et magnétiques. L'analyse des données associe la sismicité régionale (sismicité historique et instrumentale) à des mécanismes focaux extraits de la carte sismotectonique de l'Afrique publiée récemment. Nous mettons en évidence des failles transformantes actives, les zones de fractures Chain (ZFC), Romanche (ZFR), Saint Paul (ZFSP) et Arkhangelskiy (ZFA). Nous calculons également les vitesses de déformation le long de ces failles du Crétacé supérieur (~85 Ma) au présent en utilisant des données paléomagnétiques et obtenons les vitesses de glissement à partir de données de moment sismique. Les vitesses de déformation montrent une première tendance stable à environ 2 cm/an, pour ensuite augmenter à 4 cm/an dans les 10 derniers millions d'années. La comparaison des vitesses de déformation au Quaternaire supérieur et des vitesses de déformation obtenues par la géodésie fait ressortir une accumulation d'énergie sismique qui pourrait mener au déclenchement d'un séisme de Mw 7–7,5 le long de la faille transformante Saint Paul. Notre analyse sismotectonique établit un lien clair entre la tectonique océanique et la tectonique continentale, qui comprend une rotation antihoraire d'environ 20°–30° des directions de la ZFC, de la ZFR et de la ZFSP. Le potentiel de grands tremblements de terre dans le golfe de Guinée devrait être pris en considération pour établir une évaluation réaliste du risque sismique et de tsunami dans le golfe de Guinée. [Traduit par la Rédaction]

Mots-clés : Afrique de l'Ouest, Golfe de Guinée, failles transformantes, évaluation de l'aléa sismique.

Introduction

Transform faults are major tectonic structures often characterized by large earthquakes (Mw > 6) with significant coseismic horizontal movements. Also called fracture zones and either continental or oceanic, these major faults are often considered as plate boundaries and the locus of important seismic strain rates and active deformation (Wilson 1965; Brune 1968; Le Pichon and Hayes 1971). The Atlantic Ocean expanded along these transform faults, particularly in its southern part where they show the physiographic connection between the northeast Brazilian shield and West African margins in the Gulf of Guinea (GOG). The intersection of the oceanic fracture zones with the African margin and continental faults was suggested for the South Atlantic region (Francheteau and Le Pichon 1972). However, the GOG region is thought to be a "stable" province from a tectonic and seismic point of view, with major structures being linked to the pan-African Proterozoic orogen (Langer et al. 1987; Antobreh et al.

Received 12 December 2018. Accepted 2 April 2019.

Paper handled by Ali Polat.

M. Meghraoui and P. Bernard. Institut de Physique du Globe de Strasbourg, CNRS–UMR 7516, France.
P. Amponsah. National Data Centre, National Nuclear Research Institute, Ghana Atomic Energy Commission, Accra, Ghana.
B. Ateba. Institute of Geological and Mining Research, Yaounde, and Mount Cameroon Volcano Observatory, Buea, Cameroon.
Corresponding author: Mustapha Meghraoui (email: m.meghraoui@unistra.fr).

[1]This paper is part of a Special issue entitled "Understanding tectonic processes and their consequences: a tribute to A.M. Celâl Şengör".

Fig. 1. Historical seismicity (box with date for largest pre-1900 event) (Table 1) (Ambraseys and Adams 1986; Amponsah et al. 2012; Rouland et al. 2016) of the Gulf of Guinea region as an excerpt of the Seismotectonic Map of Africa (Meghraoui et al. 2016). Locations of 1855 and 1878 earthquakes are from Ambraseys and Adams (1986). The instrumental seismicity (circle) is from 1900 up to 2014 (compiled in Meghraoui et al. 2016) and from 2014 to first quarter of 2017 (International Seismological Centre 2017; Di Giacomo et al. 2014). Arrows indicate from north to south the Arkhangelsky, Saint Paul, Romanche, and Chain transform faults (see also Fig. 2). The Saint Paul, Romanche, and Chain transform faults are hidden below sedimentary cover near the African coastline. Focal mechanisms are from CMT-Harvard and the bathymetry and topography are from GEBCO (Smith and Sandwell 1997). [Colour online.]

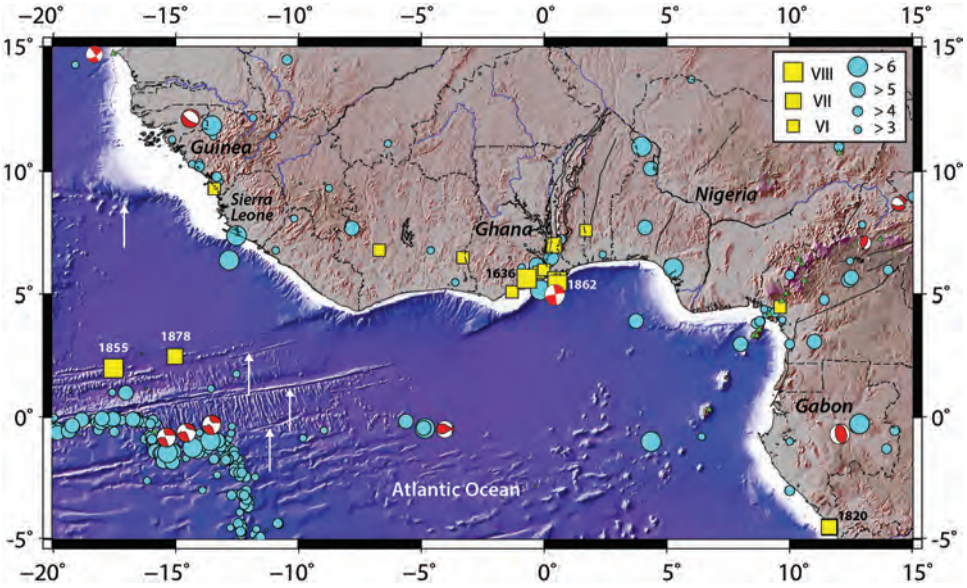

2009). Although evidence of faulted Quaternary units exists in seismic profiles (Riboulot et al. 2012), the active tectonics along major transform faults have been poorly investigated. This region has been affected by several major earthquakes over the last four centuries (Fig. 1). Among the major seismic events, the Accra earthquake of 22 June 1939 (Mw = 6.5) caused significant human and material damage (Langer et al. 1987; Kutu 2013; Meghraoui et al. 2016). While transform faults in the GOG may generate large earthquakes with coastal impacts and damage, their segmentation and seismic strain rate are poorly known.

The seismic activity inland seems to be linked to the reactivation of Paleozoic and Proterozoic tectonic structures of the West African geology (Ambraseys and Adams 1986). However, this activity appears to be in continuation of the oceanic transform faults in the GOG (Kutu et al. 2013). The seismic activity along the transform fault of the GOG can be compared to the Gloria transform fault that links the Azores triple junction in the mid-Atlantic Ocean with the Gibraltar Straight and North Africa active zone. The Gloria fault was responsible for several large earthquakes and among them the 1 November 1755 Lisbon earthquake and the 25 November 1941 seismic events reaching a magnitude larger than 8.0 generating a tsunami (Grimison and Chen 1986; Baptista et al. 1998; Batista et al. 2017). In the GOG, the historical seismicity catalogue since the 17th century reports the occurrence of several large seismic events reaching Mw 6.5 that can be related to the Romanche, Chain, and Saint Paul transform faults (Ambraseys and Adams 1986; Amponsah et al. 2012; Rouland et al. 2016).

In this paper, we explore the active tectonics and seismic behaviour of oceanic transform faults in the GOG and their continuation in continental Africa based on the recent seismotectonic analysis of West Africa and related margin. We compile previous works on active faulting and seismic profiles and present evidence of seismogenic faulting using a correlation between seismic (historical and instrumental catalogues and focal mechanisms), geodetic, palaeomagnetic, bathymetric–topographic, regional gravimetric, and magnetic anomaly data. This correlation initially allows the mapping of the different transform faults affecting the region, their characterization as seismogenic segments, and their continuation inland. The seismic strain rate is estimated from offshore fault offsets, paleomagnetic data, and cumulative seismic moments. The slip rate on faults is derived from the active deformation at different time scales and their comparison with the present-day geodetic strain. We also suggest a maximum magnitude of earthquakes that can be generated on these faults and their return period. Finally, we discuss the segmentation of seismogenic faults and their connection with continental tectonic structures.

Seismotectonic setting

The opening of the equatorial Atlantic Ocean is characterized by an initiation of oblique rifting until the Cretaceous period (125 Ma). This tectonic episode led to the segmentation of the Brazilian and West African cratons and the formation of the mid-Atlantic rifted margins. The latter have been affected by several transform faults and among them the Romanche fault (Fig. 1) (Antobreh et al. 2009). The regional seismotectonic context was recently studied along with the development of a database during the preparation of the Seismotectonic Map of Africa (UNESCO–IGCP-601 project: Meghraoui et al. 2016).

In the GOG region, the stress field obtained mainly from focal mechanisms (Delvaux and Barth 2010) shows a predominantly strike-slip tectonic regime, with some reverse faulting in Gabon, Cameroon, and Atlantic Sea (latitude 0°, longitude −5°) and normal faulting in Guinea and Ghana. Figure 1 and Table 1 show several large earthquakes from historical and instrumental seismicity located inshore and offshore the GOG region. The seismicity occurs also on old fault lineament of the Paleozoic bedrock that is reactivated in the Quaternary, as is notably the case in the Ghana marginal ridge (Blundell 1976; Wright 1976; Amponsah et al. 2012) and Late Quaternary stratigraphic architecture of the eastern Submarine Niger Delta. Other earthquakes such as the 11 March 1855 (Mw = 6.5) and 10 October 1878 (Mw = 6.3) offshore Liberia seem to have been initiated on one of the transform faults

Table 1. Major historical and instrumental earthquakes with Mw > 6 of the Gulf of Guinea (Fig. 1) (Ambraseys and Adams 1986; Amponsah et al. 2012; Meghraoui et al. 2016).

Earthquake event	Date	Latitude	Longitude	Mw
Gbefi, Ghana	10 July 1682	7	0.4	6.5
Offshore Monrovia Liberia (1)	11 March 1855	2	–17.5	6.5
Offshore Monrovia Liberia (2)	11 October 1878	2.5	–15	6.3
Accra, Ghana	22 June 1939	5.18	–0.13	6.5
Gabon	23 November 1974	–0.28	12.83	6.1
Mania, Sierra Leone	4 January 1957	7.4	–12.5	6.2
Gaoual, Guinea	22 December 1983	11.85	–13.5	6.2
Tungen Gendei, Nigeria	27 January 2011	11.02	3.98	6.2

of the GOG (Ambraseys and Adams 1986; Rouland et al. 2016). From a seismotectonic point of view, all of these seismic events question the stable character generally associated with the onshore and offshore West Africa region.

Several research projects in transform regions comparable to the GOG have documented the seismic behaviour of oceanic transform faults and their connection to the continental tectonic structures. The oceanic crust is older at the GOG due to the opening of the North Atlantic before the South Atlantic (Francheteau and Le Pichon 1972). One of the most noteworthy works that documents an oceanic transform fault and its continental continuity is the seismotectonic study conducted by Grimison and Chen (1986) on the Azores–Gibraltar Gloria fault. Grimison and Chen (1986) documented the focal mechanisms and depths of 10 moderate earthquakes (Mw < 6) from 1968 to 1973 and five large earthquakes (with Mw > 6) from 1954 to 1980. From the North Atlantic region, the Gloria fault extends eastward and forms the plate boundary between Eurasia and Africa in the western Mediterranean. The fault is associated with the occurrence of large earthquakes with Mw 8.5–9.0 and up to ~4 cm/year mid-Atlantic oceanic expansion rate (Burke 1969; Kreemer et al. 2014). The Gloria fault reveals a transition between ocean–ocean convergence with continental collision at passive margins of the Eurasia (Iberia) – Africa plate boundary that implies a better characterization of the seismic or aseismic character and earthquake rupture segmentation of a major transform fault.

Data and methodology

Bathymetric and topographic data

The topographic and bathymetric data extracted from GEBCO (Weatherall et al. 2015) used, have a resolution of 1 arc minute (approximately 1.5 km). This level of resolution allows us to highlight the sea-floor tectonic and geomorphological structures, such as the segmentation and termination of oceanic transform faults, which cannot be identified on low-resolution maps. The bathymetric data are taken from version 18 of the bathymetric model derived from the combination of satellite altimetry and boat depth surveys, prepared by Smith and Sandwell (1997). To increase the visualization of fault escarpments on maps, a gradient was applied to the bathymetry data. Their usefulness in this study is mainly to obtain a better visibility of the different fault zones in relation to the seismotectonic framework of the GOG (Meghraoui et al. 2016).

Magnetic data

The magnetic data used in this study are primarily the global magnetic anomaly presented in nanotesla (nT) from the EMAG2 project (Maus et al. 2009). These data were compiled from marine magnetic anomaly acquisition campaigns, land, air, and satellite. They consist of a nondirectional grid with 2 arc minutes resolution of (~3 km) at an altitude of 4 km above mean sea level. This resolution allows a clear improvement in the visualization of the world magnetic anomaly compared to previous projects and in particular compared to the EMAG3 project, dating from 2007 and related 3 arc minutes resolution (~5.5 km). For the same purpose as the bathymetry and topography data, it was decided to apply a gradient to these magnetic anomaly data. As shown by Maus et al. (2009), the higher magnetic resolution is obtained in particular for the ocean domain and is therefore the best model of magnetic anomaly applied for the identification of tectonic structures and transform faults of the oceanic lithosphere.

The timing of palaeomagnetic inversions available on the tectonic map of Africa (Milesi et al. 2010) was also used in this study to estimate deformation rates during the past geological tectonic episodes. The velocities of tectonic blocks and related fault zones were obtained measuring the displacement of the oceanic crust produced for each paleomagnetic inversion on the West Africa seafloor spreading. A deformation velocity ranging from 0.4 to 2.23 cm/year depending on the oceanic rheology (rigidity modulus) is thus inferred from palaeomagnetic inversions (C5 –9.7 Ma to inversion M4 –126.7 Ma) for the area between latitudes 5°S and 10°N and up to inversion M25 for the area between latitudes 10°N and 15°N.

Gravity data

The gravimetric data used in this study correspond to version 23 of the world Bouguer's anomaly model of the gravimetric field in milligal (mGal) developed by Sandwell et al. (2014). As for the bathymetric and topographic data, their resolution is 1 arc minute and about 2 mGal accuracy, which is a significant improvement with regards to previous models (Sandwell et al. 2014). Our main interest in using these data is the possibility of identifying tectonic and geomorphological structures whose gravimetric signals are characterized by short wavelengths. Indeed, they allow the identification of these structures even if concealed by a sediment cover as is the case in the GOG and more precisely in the Niger Delta. To better observe the anomalies on the generated maps, it was decided to limit their amplitude to 240 mGal (from –120 to 120 mGal). This amplitude limitation of the anomaly has the effect of increasing the contrast between the regional gravimetric field and the anomalies, thus allowing a better visualization of the latter. As for the bathymetry and magnetic anomaly, a gradient was applied to the gravimetric anomaly to emphasize the surface trace of the faults. A more detailed investigation of the termination of transform faults at the ocean/continent is possible using topographic, bathymetric, magnetic, and gravimetric data.

Historical seismicity

The regional historical seismicity provided in our study was obtained from the database and catalogue prepared for the Seismotectonic Map of Africa (Meghraoui et al. 2016). It corresponds to the seismicity recorded before 1900, homogenized and harmonized according to the standardized intensity scales and converted to moment magnitude (Mw). This catalogue was constructed through the research work of historical earthquakes at the regional scale and from a compilation of previous publications, reports, and

field accounts (Ambraseys and Adams 1986; Amponsah et al. 2012; Rouland et al. 2016).

Instrumental seismicity

The regional instrumental seismicity is, as for historical seismicity, provided by the catalogue used for the preparation of the seismic map of Africa for earthquakes from 1900 up to 2014 (Meghraoui et al. 2016). This catalogue was then completed thanks to the database put online by Di Giacomo et al. (2014) for the International Seismological Centre (2017) for 2015, 2016, and the first quarter of 2017 (ISC Bulletin; ISC 2014–2017). The energy of earthquakes that have occurred in the GOG region is homogenized and harmonized according to the standardized magnitudes (Ms, M_L, m_b) and converted into moment magnitude Mw (Scordilis 2006).

Focal mechanisms

Focal mechanisms used in our study are predominantly strike-slip faulting taken from the online global CMT catalogue (globalcmt.org) provided by Ekström et al. (2012) according to the methodology defined by Dziewonski et al. (1981). The catalogue thus covers the period from 1976 to 2017 for earthquakes of moment magnitude greater than 5. The interest of using these data is, in addition to the understanding of the deformation regime at the level of transform faults, the access to seismic moments of the different earthquakes. It is based on the formula of the scalar seismic moment defined by Aki (1972):

$$(1) \qquad Mo = \mu S \Delta U$$

where μ is the rigidity of the medium, S is the surface of earthquake rupture, and ΔU is the average displacement on the surface S. Hence, the summation of seismic moments of seismic events that occurred along the oceanic transform faults is then possible (Brune 1968). It provides access to the seismic deformation velocity of the study area for a given period t and in particular for short and recent time scales. The most commonly used formula is the seismic summation of Kostrov (1974):

$$(2) \qquad \dot{\varepsilon}_{ij} = \frac{1}{2\mu V t} \sum_{n=1}^{N} Mij^n$$

where $\dot{\varepsilon}_{ij}$ corresponds to the rate of geological deformation (centimetres per year), V is the crustal volume, $\Sigma M_o ij$ is the cumulative seismic moment tensor, and t is the time window in years of seismicity catalogue. This equation is thus viable if the framework corresponds to a volume. However, the media affected by deformation is in our case transform faults, which can be assimilated to planes of length L, width or thickness of seismogenic crust W, and surface $S = L \times W$. To try to quantify the deformation velocity at the level of these fault planes by directly using this formula could lead to a non-negligible error. The objective of this calculation is to estimate as precisely as possible the deformation velocity for each fault plane identified as seismogenic. The estimation volume affected by the seismogenic activity along the given fault segment must therefore be as precise as possible, although it is difficult to have access to field investigations in the GOG oceanic context. To avoid this problem and quantify the deformation velocities resulting from seismic moments for the considered time scales, the following equation resulting from a simplification of Kostrov's summation is proposed:

$$(3) \qquad \dot{U} = \frac{1}{\mu S} \dot{M}o$$

where S is the surface affected by deformation and $\dot{M}o$ is the deformation velocity resulting from the seismic moment summation. It thus makes it possible to free oneself from the limits linked to the poor knowledge of the volume affected by each fault. The slip rate obtained for each fault plane is then summed to estimate the deformation velocity using the cumulative seismic moments for the entire study area. Compared to the long-term geological velocity obtained from the cumulative displacements and related ages using paleomagnetic data, it finally allows a better understanding of the accommodation of the deformation at the fault plane level and in particular to observe whether a change of deformation regime occurs in recent times (hundreds to thousands of years) with regards to old times (million years).

Geodetic data

The geodetic data used in this study correspond to the velocity field for Africa as modeled by displacement directions (also using focal mechanisms) and global GPS and VLBI data (Kreemer et al. 2014). The geodetic velocities used in the study are shown in Fig. 2. These results were established through a network of about a hundred permanent GNSS stations coupled with a threshold value of 2.5 years. Some plate boundary velocities correspond to the most recent estimate of relative plate deformation velocities and are calculated from a treatment defined by Bos et al. (2013). In our case, the velocities used correspond to the deformation velocities of the mid-Atlantic ridge expansion. From these, a simplification of the "seismic moment deficit" is carried out by using the following equation (Murray and Segall 2002):

$$(4) \qquad \dot{M}_d = \mu \int_s \int \int \int (\dot{U}_\alpha - \dot{U}) ds$$

where $\dot{M}_d$ is the seismic moment deficit, $\dot{U}_\alpha$ is the geodetic rate between the tectonic blocks separated by the locked fault, and $\dot{U}$ is the fault slip rate based on the measured dated displacement. It is necessary to characterize the seismic moment deficit because it may give access to the seismic energy to be accommodated along a given fault zone of the GOG region. The GOG is thus characterized by two geodetic velocities, 2 cm/year in the north and 2.3 cm/year in the south of the GOG region. To respect our adopted approach, these velocities are summarized taking into account two tectonic blocks to the north and south of the faults to account for all of the cumulative deformation.

Analysis of strain distribution in the GOG

The correlation of historical and instrumental seismicity data with topography and bathymetry contributes to a better understanding of the seismotectonic structures of the GOG. In Fig. 1, the east–west-trending seismicity and topography can be correlated with the Saint Paul (SPFZ), Romanche (RFZ), and Chain (CFZ) transform faults, but the fault traces are concealed below Quaternary deposits near the African coastline. The regional gravity and magnetic anomalies show the transform fault extensions to the coastlines and related offsets of tectonic structures (Figs. 3*a*, 3*b*, and 4).

The gravity and magnetic data of the oceanic domain presented in Figs. 3*a* and 3*b* show prominent offshore fault scarps with fresh morphology in comparison with the tectonic framework presented in Fig. 1. This improvement of fault visibility is particularly accurate to the south of the Romanche fracture zone (RFZ) and indicates the structural characteristics of analogue transform faults of the GOG. Figures 3*a* and 3*b* appear to show two main types of anomalies that include small, point, and small positive gravity anomalies coupled with the positions of continental and oceanic African volcanoes that appear to correspond to the Neogene and Quaternary volcanic fields. Several rectilinear long-range negative anomalies (about a few hundred to a thousand kilometres) are then visible and therefore represent the main transform faults affecting the GOG.

Fig. 2. Geodetic expansion rates (arrow with total deformation) across the plate boundaries around Africa (Kreemer et al. 2014; Meghraoui et al. 2016). Green triangles are GPS stations in continental Africa and neighbouring islands. Bathymetry and topography are from GEBCO (Smith and Sandwell 1997). [Colour online.]

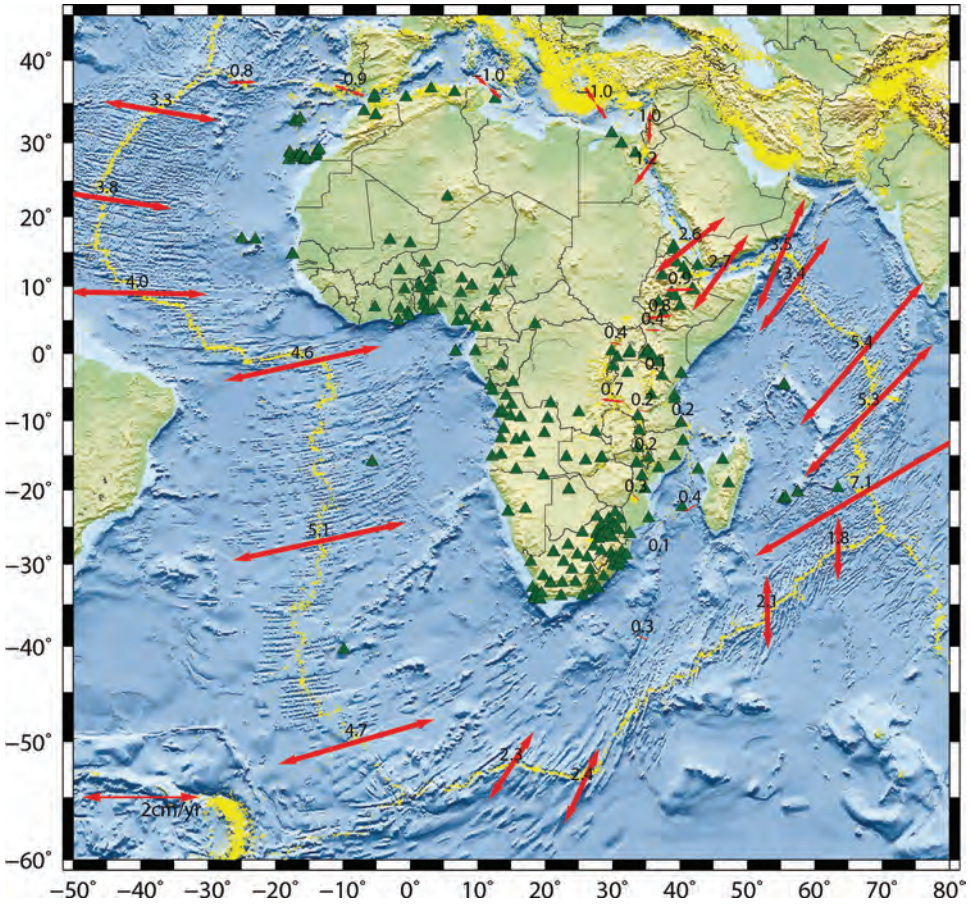

The combination of these anomalies shows a consistent superposition with the morphological traces of the bathymetric data and contributes to better visualize the fault traces under relatively thick quaternary sedimentary cover near the coastline. This is the case across the Niger Delta sedimentary basin, whose total thickness of Mesozoic, Cenozoic, and Quaternary sediments is between 8 and 12 km (Mvondo Owono 2010).

The earthquake distribution also characterizes the four main seismic fracture zones (i.e., Arkhangelskiy (AFZ), SPFZ, RFZ, and CFZ) in the GOG (see for instance Bonatti et al. 1994 for the CFZ). The four transform fault zones (Figs. 1, 3*a*, and 4) show a pattern of deformation that is consistent with the tectonic studies previously carried out on the opening of the equatorial Atlantic Ocean (Antobreh et al. 2009). Each of the transform faults of GOG has recorded moderate to large earthquakes (with Mw > 5) in the last 35 years and shows a maximum seismicity rate along the Romanche fault (see Table 2).

Crustal deformation and variable seismic strain rate

The choice of the value of the rigidity modulus μ is an important step to better estimate the rate of active deformation in the oceanic domain of the GOG. As shown in eqs. 1, 2, and 3, the rigidity modulus is a determining parameter for seismic moment calculation of earthquakes and hence the velocity of crustal deformation. The usual value of this parameter is 3.3×10^{10} N/m^2 when the medium affected by one or more earthquakes corresponds to the continental lithosphere. In our case, the study area corresponds to an oceanic lithosphere that has colder and denser rheological characteristics that match a lower rigidity modulus. In their study of the RFZ, Bonatti et al. (1994) recommend a Young Modulus E = 60 GPa and a dimensionless Poisson coefficient ν = 0.25, consistent with those of a basaltic rock (Handin and Carter 1987). Thus, the presumed nature of the upper part of the oceanic crust may vary and have different physical properties.

Considering the following equation:

$$\mu = E2(1 + \nu) \quad (5)$$

The value obtained for μ is 2.6×10^{10} N/m^2. Our calculation of the cumulative moment rate and seismic slip deficit is obtained taking into account both values of rigidity modulus with $\mu_1 = 2.6 \times 10^{10}$ N/m^2 and $\mu_2 = 3.3 \times 10^{10}$ N/m^2.

Correlation with continental structures

To better understand the possible role of oceanic transform faults in crustal deformation and associated seismic activity in the GOG, it is important to first study their eastern endings. The influence of fracture zones in the GOG on seismicity was also assumed by Burke (1969), especially on the Guinean coast, as early as the 1960s. The connection between oceanic and continental structures is hence made through the 2000 m high fault scarp of the Ivory Coast – Ghana continental marginal ridge (Mascle and Blarez 1987; Delteil et al. 1974; Blundell 1976). More recent studies with seismic profiles and detailed seafloor deformation highlight the alignment of continental tectonic structures such as the Akwapim fault zone in Ghana with the RFZ (Guiraud et al. 1997; Edwards et al. 1997). In the Guinean coast, where the RFZ is termi-

Fig. 3. (*a*) Gravity anomaly (Sandwell et al. 2014) and regional seismicity (Meghraoui et al. 2016; box for historical, circle for instrumental). We observe that in contrast with Fig. 1, the Saint Paul, Romanche, and Chain transform faults can be traced clearly until they reach the African coastline. Focal mechanisms are CMT-Harvard. (*b*) Detail of gravity anomaly of Fig. 3*a* with a focus on the eastern end of the Romanche transform fault (arrow). The offshore 2200 m high scarp forms the marginal ridge that connects with the continental Akwapim fault zone south of Accra (Ghana) (Blundell 1976; Guiraud et al. 1997). Farther south, the eastern end of the Chain transform fault (arrows) crosses the Niger delta and expose faulted Quaternary deposits (Riboulot et al. 2012). Seismicity (circle and box) is as in Fig. 1 and triangles mark the Cameroon volcanic line. [Colour online.]

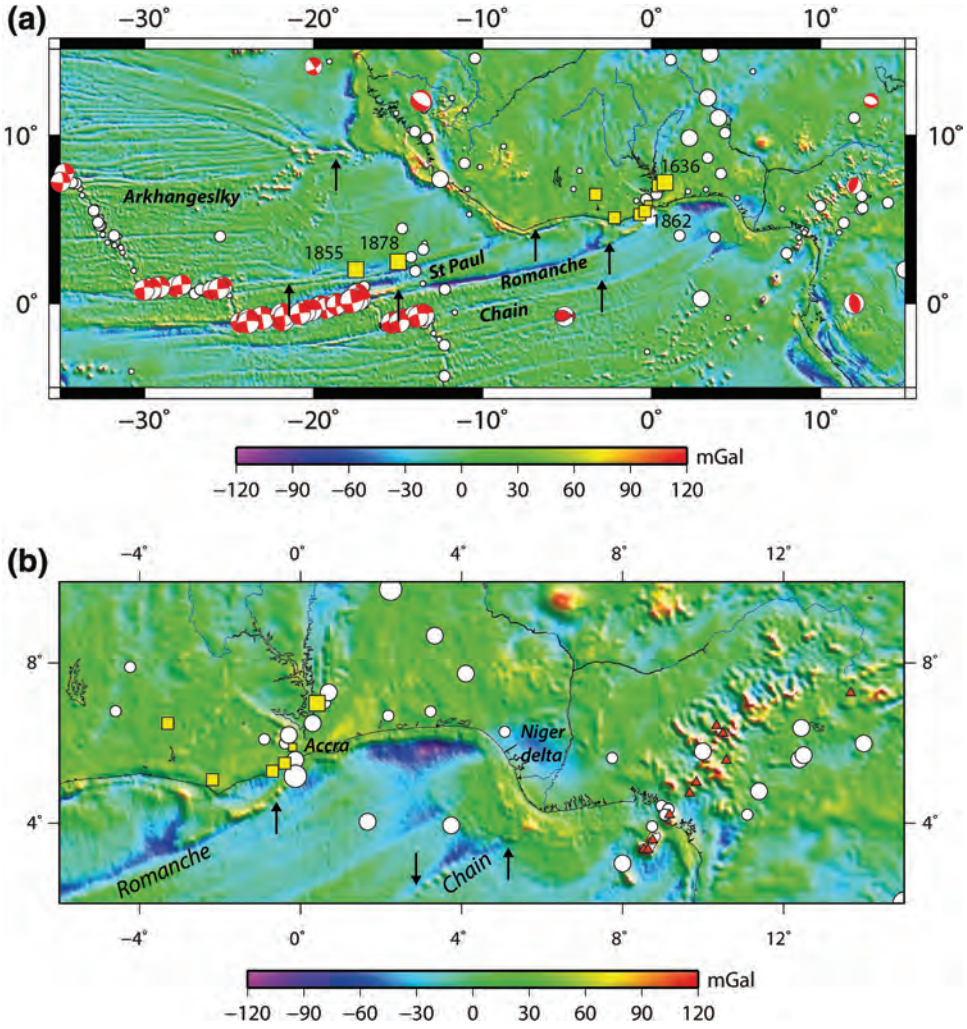

nated, recent tectonic studies in the region are increasingly highlighting the interaction of continental structures with RFZ, such as the Akwapim, Adina, and Fenyi–Yakoe faults in Ghana. Indeed, it has recently been shown that these faults may be linked to continental terminations of the RFZ in the Keta Cenozoic basin (Amponsah et al. 2012). In addition, previous studies show that the Accra earthquake of 22 June 1939 (Mw = 6.5) occurred about 40 km off the coast of Ghana (position: 5°11′N, 0°8′W; Kutu et al. 2013) and could be initiated at the junction between the Romanche oceanic fault and Akwapim continental fault zone (Blundell 1976). This work also highlights the presence of escarpments of continental faults linked to this earthquake whose epicentre is oceanic (which would prove that the epicentral location is approximate). This latter point would thus suggest an interaction between these continental faults and the RFZ for seismic activity in the Accra region, which lies between the Birimian and Dahomeyan tectonic blocks (Blundell 1976). In addition, the correlation between continental and oceanic tectonic structures for RFZ (Wright 1976) seems to confirm the occurrence of the 11 September 2009 (Mw 4.2) earthquake in southwest Nigeria. The latter study indicates an epicentre very close to the RFZ and has resulted in the reactivation of cracks affecting the Precambrian basement in a compressive context (Akpan et al. 2009).

A coupled plastic and elastic deformation in the brittle lithospheric plate may trigger earthquakes, implying stress transfer with displacement continuity along fault zones (Lin and Parmentier 1989). The mechanism of crustal fault propagation with stress transfer from the oceanic domain across the continental shelf may explain the link between the oceanic transform faults and continental faults (e.g., between the Romanche fracture the Akwapim fault zone). Other earthquakes also seem to indicate a possible stress transfer between the oceanic and continental domains at other fault/fracture zones. For example, the Gaoual–Guinea earthquake of 22 December 1983 (Mw 6.2; see Table 1 and Figs. 1 and 3), characterized by the reactivation of preexisting continental faults, is in line with several oceanic transform faults, including AFZ (Langer et al. 1987). The Mania earthquake in Sierra Leone on 4 January 1957 (Mw 6.2; see Table 1 and Fig. 1) is also a continuation of the AFZ. This coastal earthquake activity suggests a possible correlation between the continental and oceanic transform faults at the West African margin.

Fig. 4. Magnetic anomaly (Maus et al. 2009) and regional seismicity (Meghraoui et al. 2016; box for historical, circle for instrumental with legend similar to Fig. 1). East–west-trending focal mechanisms (CMT-Harvard) delineate the transform faults. The red triangle is a volcanic crater. As for gravity anomalies of Figs. 3*a* and 3*b*, magnetic anomalies mark the main transform fault zones extending eastward from the mid-Atlantic ridge to the African coastline. [Colour online.]

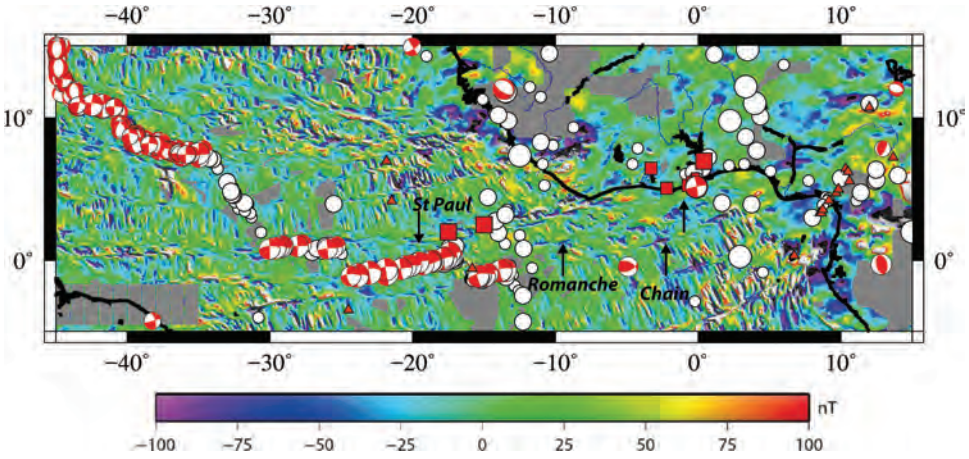

Table 2. Seismogenic faults and related characteristics with fault length, thickness of seismic layer, and maximum earthquake magnitude recorded in the last 35 years along respective fault.

Seismogenic fault zone (from south to north)	Length of seismogenic fault plane (km)	Thickness of seismogenic crust (km)	Largest event with recorded magnitude
Chain	211±36	3–11	28 August1992 Mw 6.8
Romanche	834±72	7–20	29 August 2016 Mw 7.1
Saint Paul	564±25.5	16±9	10 December 1996 Mw 6.68
Arkhangelsky	572±65.7	15.12±9.5	1 November 1984 Mw 7

Note: Uncertainties in fault length are obtained from the maximum magnitude inferred from fault length (Hanks and Kanamori 1979; Wells and Coppersmith 1994). Uncertainties in the seismogenic layer are estimated from the seismicity distribution and body wave inversion along fault zones (Abercrombie and Ekström 2001; Ekström et al. 2012).

Further studies have been conducted to better understand the transition between the oceanic and continental crust in the GOG. The most notable work is that of Davies et al. (2005) who undertook a 3D modeling of the eastern termination of the CFZ and suggested a transitional crust as the ocean–continent boundary. Seismic profiles performed across the southern Niger delta show faulted Late Quaternary deposits that attest for active tectonics along the Chain transform fault (Riboulot et al. 2012). Further north, and despite the lack of seismic profiles and instrumental seismicity, the seismogenic region of Axim–Elmina in Ghana may be linked to the reactivation of the SPFZ (Kutu 2013). Due to the quiet character of this fault along strike near the coastline, an acquisition of seismic profiles could be an alternative to characterize the ocean–continent transition.

It is also necessary to refer to the tectonics of the Brazilian passive margin where its history is indeed linked to that of West Africa (Le Pichon and Hayes 1971). These two margins have been affected by the same oceanic transform faults. In particular, the work of Gomes et al. (2000) led to a better understanding of the ocean–continental transition at the north-northeast part of the Brazilian margin. This work revealed a transitional crust characterized by the presence of the Pernambuco and Rio Grande do Norte plateaux, which corresponds to a thin and extensive continental crust (Gomes et al. 2000). This type of transitional crust is also found in the GOG and more precisely in the Niger Delta (Davies et al. 2005). Another common point with the GOG is the presence of northeast–southwest-orientated volcanic fields comparable, for example, to the volcanic line of Cameroon. These fields are also thought to be related to the tectonic activity of transform faults affecting the north-northeast margin of Brazil (Gomes et al. 2000). A tectonic reactivation of the fracture zones would have taken place following magmatic activity due to a hot spot. The acquisition of seismic profiles at the level of these faults also makes it possible to characterize their morphology, marked by large discrepancies between the various crustal segments at the margin level (Gomes et al. 2000).

Discussion

Comparison of long-term geological rate, seismic strain rate and seismic moment deficits

As stated previously, the deformation velocities resulting from the seismic moments were summarized and compared with the deformation velocities obtained using paleomagnetic inversion as well as geodetic velocities by following eqs. 3 and 4. The earthquake ruptures were derived from the parameters of Table 2. The timing parameters for the calculation of elastic velocities (using the summation of seismic moments), seismic moment, and the results of velocity calculations and seismic slip deficits are shown in Tables 3 and 4. The total deformation rate resulting from the summation of the seismic and geodetic moments for the GOG are, respectively, 5.5 cm/year if $\mu = 2.6 \times 10^{10}$ N/m^2 and 4.1 cm/year if $\mu = 3.3 \times 10^{10}$ N/m^2.

The estimated fault slip rates of Table 3 allowed the construction of the velocity graph (Fig. 5) obtained using eq. 3 for the four seismogenic transform faults of the GOG. The graph shows the summation velocities of the seismic moments for both $\mu = 2.6 \times 10^{10}$ and 3.3×1010^{10} N/m^2. From a first observation, the graph shows that the velocities obtained from paleomagnetic inversion data have the same trend for the four transform faults. They all have an oceanic crust expansion rate of ~2 cm/year from the South Atlantic opening marked by paleomagnetic inversion M0 to

Table 3. Cumulative seismic moment and slip rate elastic velocity for two different rigidity moduli μ and for each transform fault zone of the Gulf of Guinea region.

Transform fault zone (from south to north)	Elapsed time (years)	Cumulative seismic moment (10^{25} dyn·cm)	Slip rate (elastic) $\mu = 2.6 \times 10^{11}$ dyn/cm^2	Slip rate (elastic) $\mu = 3.3 \times 10^{11}$ dyn/cm^2
Chain	39	6.56	1.81	1.2
Romanche	38	31.3	2.23	1.7
St. Paul	39	5.07–6.12 (including historic seismicity)	0.55	0.4
Arkhangelsky	39	8.87	1.01	0.8

Note: Seismicity data are for the 1900–2017 period (Ambraseys and Adams 1986; Amponsah et al. 2012; Meghraoui et al. 2016) (see also Fig. 1).

Table 4. Geodetic rate (Kreemer et al. 2014) and seismic deficit for two different rigidity modulus μ and for each transform fault zone of the Gulf of Guinea region.

Transform fault zone (from south to north)	Geodetic rate (cm/year)	Seismic slip rate deficit (cm/year) if $\mu = 2.6 \times 10^{11}$ dyn/cm^2	Seismic slip rate deficit (cm/year) if $\mu = 3.3 \times 10^{11}$ dyn/cm^2
Chain	2.3	0.49	1.1
Romanche	2.3	0.07	0.6
St. Paul	2.3	1.75	1.9
Arkhangelsky	2.0	0.99	1.2

Fig. 5. Slip rate of the four transform faults Arkhangelskiy fault, St. Paul fault zone, Romanch fault zone, and Chain fault zone of the Gulf of Guinea estimated from paleomagnetic data (Milesi et al. 2010). Deformation rates from the cumulative moment summation are here linked to the Romanche fault zone. The square indicates the cumulative geodetic rate in the Gulf of Guinea (Kreemer et al. 2014). [Colour online.]

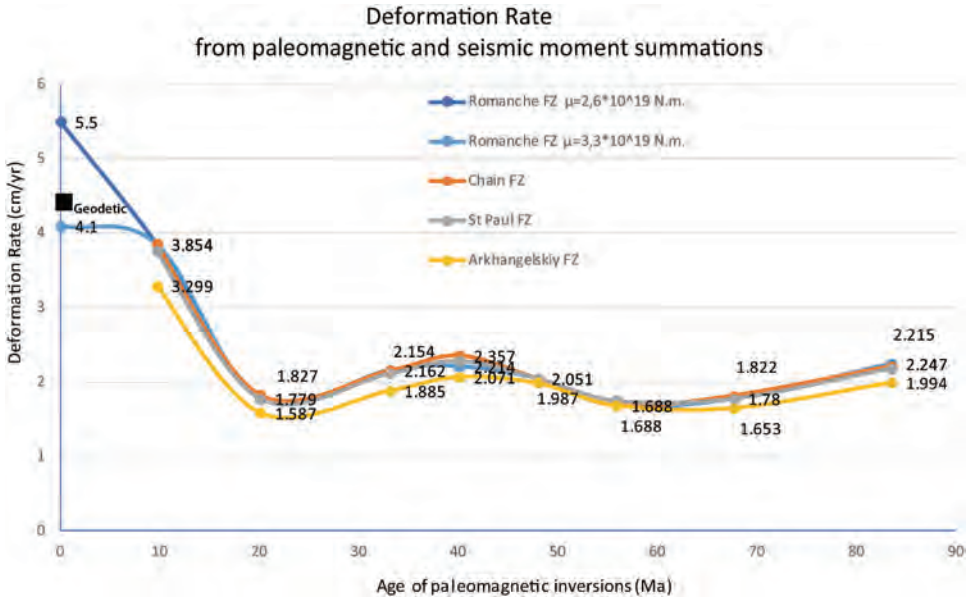

Chron 6 (20.1 Ma). An acceleration of this expansion rate of up to 3.9 cm/year is then performed from Chron 5 (9.7 Ma) to the current one. The lack of resolution of the most recent paleomagnetic inversion in the GOG does not allow us to calculate deformation velocities based only on paleomagnetic data (Milesi et al. 2010).

The current velocities resulting from the seismic moment summation show in a first case a continuation of the acceleration of the deformation velocity along the transform faults ($\mu = 2.6 \times 10^{10}$ N/m^2) up to a cumulative 5.05 cm/year (Table 3; Fig. 5). The second configuration indicates a cumulative deformation velocity of 4.1 cm/year. The geodetic velocity affecting the GOG (Kreemer et al. 2014) represented in Fig. 5 by the black rectangle has a value of 4.3 cm/year comparable to the slip rate value of the second configuration. The seismic moment deficits calculated here according to eq. 4 and the two possible models show variable results. Indeed, considering $\mu = 2.6 \times 10^{10}$ N/m^2, the deficits of the CFZ and AFZ seem to show a seismic strain rate that does not accommodate part of the deformation. Similarly, the seismic activity of the SPFZ would not accommodate a large part of the deformation. Thus, there would be a medium (CFZ and AFZ) to high (SPFZ) accumulation of deformation at these faults. With regard to the RFZ, the value of its deficit would be almost zero (0.07), which would mean that its seismic activity would almost entirely accommodate the deformation along the fault itself and the accumulation of deformation through the fault would therefore be very small. If a value of $\mu = 3.3 \times 10^{10}$ N/m^2 is taken into account, the seismic slip rate deficit increases for all faults from 0.49 to 1.1 cm/year for the CFZ, from 0.07 to 0.6 cm/year for the RFZ, from 1.75 to 1.9 cm/year for the SPFZ, and from 0.99 to 1.2 cm/year for the AFZ.

In this model, a non-negligible accumulation of deformation for recent times would occur for all four faults of the GOG. However, if the RFZ, CFZ, and AFZ show relatively significant variations in the value of the seismic slip deficit, the SPFZ shows a strong accumulation of seismic strain. The SPFZ also has similar values for the models (1.75 and 1.9 cm/year) (Table 4). If for seismic hazard estimation purposes, a 50 year period is considered, this accumulation of deformation would be equivalent to a displacement of 87.5–95 cm. According to the scaling relations of Wells

and Coppersmith (1994), this displacement would correspond to an Mw ~7 earthquake. If the period considered is a century, this displacement would be between 1.75 and 1.9 m, which would be equivalent to an earthquake of Mw ~7.5. It would then be a major earthquake with a break in the order of 100 km, which, depending on its epicenter position, could damage coastal cities and even generate destructive tsunami waves.

However, several points need to be addressed to validate the possibility of the occurrence of such a large earthquake. First, a better knowledge of the rheology of the regional upper crust would allow a better characterization of the upper crust stiffness modulus. The absence of geodetic data makes it impossible to determine precisely the geodetic deformation velocity of the region and thus the deficiency of the seismic moment. A point of improvement to better understand the accommodation of deformation at these fault planes could be the calculation of the true seismic moment deficiency (in dyne centimetres per year) at the fault plane using the geodetic velocity field. The moment deficit $\dot{M}d$ given by eq. 4 (Murray and Segall 2002) allows estimation of the interseismic time ti between two earthquakes according to the following equation:

$$ti = Mo/\dot{M}d \quad (6)$$

It would then be possible to estimate with this equation the time required for the elastic deformation to be released into the crustal volume surrounding the fault zone.

Fault segmentation

An important point in understanding the fault structures and the propagation of seismic ruptures along strike is the understanding of their segmentation and the organization of geometric and structural discontinuities. For the continental domain, the fault identification and characterization involves field investigations coupled with the examination of aerial photographs and satellite images. For the oceanic domain, the geometrical discontinuities along faults depend on the resolution of bathymetric, gravimetric, and magnetic data. Although these data could be sufficient to identify the various fault zones, they do not allow us to accurately characterize their segmentation. To estimate the structural characteristics and segmentation of these transform faults, it is possible to use the scaling laws defined by Hanks and Kanamori (1979) and inferred by Wells and Coppersmith (1994), which are mainly based on the length of coseismic ruptures and the moment magnitudes of the associated earthquakes. A major issue, however, is the thickness of the seismogenic layer that may change in the oceanic crust from a relatively thin layer (~8 km) to a relatively thick layer (21 km) along the transform faults. In their study of the seismic source characteristics, Abercrombie and Ekström (2001) obtained 7–20 and 3–11 km hypocentre depths for the Romanche and Chain fault ruptures; in addition, they showed from body wave inversion of the 1994 earthquake (Mw 7.1) that the slip distribution may reach ~2 m at the surface along a ~120 km long fault rupture.

Taking into account the seismic source dimensions along the RFZ and largest recorded earthquakes (26 December 1992 Mw 6.8, 14 March 1994 Mw 7.1, and 21 December 2003 Mw 6.5), it is then possible to infer the number of segments making up the fault and their respective lengths from earthquakes of magnitude Mw ≥ 6.5, assuming that such earthquakes can be initiated homogeneously on the fault. In our case, this hypothesis would be supported by the presence of seismicity all along the transform faults, as is notably the case with SPFZ or with the possible stress transfer along the RFZ. Mw magnitudes of fault segments are close to, or equal, to 7 for the largest earthquakes associated with each active transform fault (see Table 2). According to Hanks and Kanamori (1979) and Wells and Coppersmith (1994), these magnitudes imply a rupture length of 60–120 km. These fault rupture lengths would then imply about 10–14 segments for RFZ, 2–4 segments for CFZ, and 8–10 segments for SPFZ and AFZ.

Open questions remain, however, on the location of geometrical discontinuities and segment boundaries and on the amount of aseismic slip along transform faults. Taking into account the 25 year Harvard CMT catalogue for large earthquakes, Abercrombie and Ekström (2001) inferred that the aseismic slip may reach half of the total seismic strain release along the Romanche and Chain transform faults. The aseismic versus seismic slip depends closely on the thickness of the seismogenic layer and its crustal rigidity (Table 2) as well as the level of seismic coupling along the transform fault segments. Using the seismicity catalogue (1900–2014) combined with the ISC and Harvard-CMT catalogue (1976–2017) (Fig. 1) and for two different rigidity moduli, the seismic slip rate may vary from 1.7 to 2.23 cm/year, which is comparable with the 1.8 cm/year inferred rate by Abercrombie and Ekström (2001). As noted in Table 4, the average 2.3 cm/year geodetic rate suggests that the largest seismic slip deficit is along the SPFZ and the lowest seismic slip deficit on the RFZ. This contingent distribution of slip deficit and seismic strain deformation in the past century or so may contribute to our understanding of the seismic behaviour of transform faults in the GOG.

Return periods for strong earthquakes

The estimation of a return period of major earthquakes (Mw > 7) is important for the regional seismic hazard assessment and quantification of the seismic risk, since the last major regional earthquake such as that of Accra on 22 June 1939 caused significant human and material damage (Kutu et al. 2013). The relatively low level of seismic activity in the GOG (in the last 50 years) prevents us from pointing out the frequency of different magnitudes according to Gutenberg–Richter law. However, one can study the time elapsed between the last earthquake with a magnitude greater than 6 for each fault using the respective seismic catalogues (ISC 2017). Thus, 22 years have elapsed for the RFZ between the last two major earthquakes (two events of Mw 7.1 in 2016 and 1994), 11 years for the CFZ (from 1992 and 2003), 11 years for SPFZ (from 1985 to 1996), and 23 years for the AFZ (from 1984 to 2007). An average recurrence of major earthquakes lasting ~17 years seems to occur at the level of the GOG faults. In contrast with historical and damaging earthquakes (Table 1), it must also be taken into account that most of recent earthquakes occurred at the level of the midoceanic ridge and hence at a great distance from the continent. The occurrence of large earthquakes along eastern sections of the transform faults closer to the coastline would be potentially damaging and be the source of tsunami waves.

Conclusion

This study focuses on the seismic behaviour of oceanic transform faults of the GOG, motivated by the recent seismotectonic analysis in the region (Meghraoui et al. 2016) and other similar transform faults (Grimison and Chen 1986). Correlation of seismic, geodetic, bathymetric, magnetic, paleomagnetic, and gravimetric data has improved the mapping of transform faults in the GOG. The four transform faults, namely the CFZ, RFZ, SPFZ, and AFZ, could also be characterized as seismogenic. The seismicity catalogue used in our study further shows that each of these faults recorded an earthquake of moment magnitude Mw ~7 over the past 33 years.

Paleomagnetic data and cumulative seismic moments have also allowed the calculation of deformation velocities from the Upper Cretaceous (~85 Ma) to the present according to two rheological models, the former having a rigidity modulus μ of 3.3×10^{10} N/m^2 and the latter a value of μ equal to 2.6×10^{10} N/m^2. The velocity calculations based on paleomagnetic inversion data thus seem to show a tendency to accelerate deformation velocities over the last

10 million years at the level of transform faults in the GOG. Considering $\mu = 2.6 \times 10^{10}$ N/m^2, the current velocities obtained by summing seismic moments would confirm this acceleration, while a value of 3.3×10^{10} N/m^2 would indicate a stabilization of the deformation velocity at approximately 4 cm/year, which is also indicated by the geodetic data. However, the two models, by comparison of geodetic and geological velocities, seem to show a strong accumulation of energy in the SPFZ. This accumulation could thus lead to the initiation of a major earthquake of moment magnitude Mw equal to 7 or even 7.5, which could lead to significant human victims and material damage in the region, given the latest major regional earthquake. This last point is all the more important, since several tectonic and seismotectonic works (Francheteau and Le Pichon, 1972; Wright 1976; Blundell 1976; Riboulot et al. 2012; Kutu et al. 2013; Amponsah et al. 2012; Meghraoui et al. 2016) infer a connection between continental tectonics and CFZ, RFZ, and SPFZ oceanic transform faults. The SPFZ would thus be linked to the seismic region of Axim–Elmina in Ghana and seismic energy could be transmitted as a stress transfer between the oceanic and continental domains. Coupled with the apparently important return period of the major earthquakes (Mw 7) highlighted by the seismic catalogue, the possible occurrence of such a large seismic event in the SPFZ would be a crucial point to be taken into account in the estimation of the regional seismic hazard.

Acknowledgements

All authors are glad to contribute to the special issue dedicated to Prof. A.M.C. Şengör. The authors are thankful to the reviewer Alassandro Valentini and an anonymous reviewer for their comments on an earlier version of the manuscript. We also thank Rui Manuel Fernandes for help in preparing Fig. 2. Discussions with Vunganai Midzi helped in improving the manuscript presentation. This work is prepared in the frame of the IGCP-659 (UNESCO) project on the Seismic Hazard and Risk in Africa. Some of the figures were prepared using the public domain GMT software (Wessel and Smith 1998).

References

Abercrombie, R.E., and Ekström, G. 2001. Earthquake slip on oceanic transform faults. Nature, **410**: 74–77. doi:10.1038/35065064. PMID:11242043.

Aki, K. 1972. Scaling law of earthquake source time-function. Geophysical Journal International, **31**: 3–25. doi:10.1111/j.1365-246X.1972.tb02356.x.

Akpan, O.U., Isogun, M.A., Yakubu, T.A., Adepelumi, A.A., Okereke, C.S., Oniku, A.S., and Oden, M.I. 2009. An Evaluation of the 11th September, 2009 Earthquake and Its Implication for Understanding the Seismotectonics of South Western Nigeria. Open Journal of Geology, **4**: 542–550.

Ambraseys, N.N., and Adams, R.D. 1986. Seismicity of West Africa. Annales Geophysicae, **4B**: 679–702.

Amponsah, P., Leydecker, G., and Muff, R. 2012. Earthquake Catalogue Of Ghana For The Time Period 1615–2003 With Special Reference To The Tectono-Structural Evolution Of South-East Ghana. Journal of African Earth Sciences, **75**: 1–13. doi:10.1016/j.jafrearsci.2012.07.002.

Antobreh, A.A., Faleide, J.I., Tsikalas, F., and Planke, S. 2009. Rift-Shear Architecture And Tectonic Development Of The Ghana Margin Deduced From Multichannel Seismic Reflection And Potential Field Data. Marine and Petroleum Geology, **26**: 345–368. doi:10.1016/j.marpetgeo.2008.04.005.

Baptista, M.A., Miranda, P.M.A., Miranda, J.M., and Mendès Victor, L. 1998. Constrains on the source of the 1755 Lisbon tsunami inferred from numerical modelling of historical data. Journal of Geodynamics, **25**: 159–174. doi:10.1016/S0264-3707(97)00020-3.

Batista, L., Hübscher, C., Terrinha, P., Matias, L., Afilhado, A., and Lüdmann, T. 2017. Crustal structure of the Eurasia–Africa plate boundary across the Gloria Fault, North Atlantic Ocean. Geophysical Journal International, **209**: 713–729. doi:10.1093/gji/ggx050.

Blundell, D.J. 1976. Active faults in West Africa. Earth and Planetary Science Letters, **31**: 287–290. doi:10.1016/0012-821X(76)90221-1.

Bonatti, E., Ligi, M., Gasperini, L., Peyve, A., Raznitzin, Y., and Chen, Y.J. 1994. Transform Migration And Vertical Tectonics At Romanche Fracture Zone, Equatorial Atlantic. Journal of Geophysical Research: Solid earth, **99**: 21779–21802.

Bos, M.S., Fernandes, R.M.S., Williams, S.D.P., and Bastos, L. 2013. Fast Error Analysis Of Continuous GNSS Observations With Missing Data. Journal of Geodesy, **87**: 351–360. doi:10.1007/s00190-012-0605-0.

Brune, J.N. 1968. Seismic moment, seismicity, and rate of slip along major fault zones. Journal of Geophysical Research, **73**: 777–784. doi:10.1029/JB073i002p00777.

Burke, K. 1969. Seismic Areas of the Guinea coast where Atlantic fracture zones reach Africa. Nature, **222**: 655–657. doi:10.1038/222655b0.

Davies, R.J., MacLeod, C.J., Morgan, R., and Briggs, S.E. 2005. Termination of a fossil continent-ocean fracture zone imaged with three-dimensional seismic data: The Chain Fracture Zone, eastern equatorial Atlantic. Geology, **33**: 641–644. doi:10.1130/G21530AR.1.

Delteil, J.R., Valery, P., Montadert, C., Fondeur, C., Patriat, P., and Mascle, J. 1974. Continental margin in the northern part of the gulf of Guinea. *In* Geology of Continental Margins. *Edited by* C.A. Burk and C.L. Drake. New York: Springer, pp. 297–311.

Delvaux, D., and Barth, A. 2010. African stress pattern from formal inversion of focal mechanism data. Implications for rifting dynamics. Tectonophysics, **482**: 105–128.

Di Giacomo, D., Storchak, D.A., Safronova, N., Ozgo, P., Harris, J., Verney, R., and Bondár, I. 2014. A New ISC Service: The Bibliography of Seismic Events. Seismological Research Letters, **85**: 354–360. doi:10.1785/0220130143.

Dziewonski, A.M., Chou, T.-A., and Woodhouse, J.H. 1981. Determination of earthquake source parameters from waveform data for studies of global and regional seismicity. Journal of Geophysical Research: Solid Earth, **86**: 2825–2852. doi:10.1029/JB086iB04p02825.

Edwards, R.A., Whitmarsh, R.B., and Scrutton, R.A. 1997. Synthesis of the crustal structure of the transform continental margin off Ghana, northern Gulf of Guinea. Geo-Marine Letters, **17**: 12–20. doi:10.1007/PL00007202.

Ekström, G., Nettles, M., and Dziewoński, A.M. 2012. The global CMT project 2004-2010: Centroid-moment tensors for 13,017 earthquakes. Physics of the Earth and Planetary Interiors, **200–201**: 1–9. doi:10.1016/j.pepi.2012.04.002.

Francheteau, J., and Le Pichon, X. 1972. Marginal fracture zones as structural framework of continental margins in the South Atlantic Ocean. Journal of Geophysical Research, **56**: 991–1007.

Gomes, P.O., Gomes, B.S., Palma, J.J.C., Jinno, K., and de Souza, J.M. 2000. Ocean-Continent Transition And Tectonic Framework Of The Oceanic Crust At The Continental Margin Off NE Brazil: Results Of LEPLAC Project. Geophysical Monograph Series, **115**: 261–291.

Grimison, N.L., and Chen, W.-P. 1986. The Azores-Gibraltar Plate Boundary: Focal Mechanisms, Depths Of Earthquakes, And Their Tectonic Implications. Journal of Geophysical Research, **91**: 2029–2047. doi:10.1029/JB091iB02p02029.

Guiraud, M., Benkhelil, J., Mascle, J., Basile, C., Mascle, G., Bouillin, J.P., and Cousin, M. 1997. Synrift to syntransform deformation along the Côte d'Ivoire–Ghana transform margin: evidence from deep-sea dives. Geo-Marine Letters, **17**: 70–78. doi:10.1007/s003670050010.

Handin, J., and Carter, N. 1987. Rheology Of Rocks. *In* Structural Geology and Tectonics. Encyclopedia of Earth Sciences, pp. 656–668.

Hanks, T.C., and Kanamori, H. 1979. A Moment Magnitude Scale. Journal of Geophysical Research, **84**: 2348–2350. doi:10.1029/JB084iB05p02348.

International Seismological Centre (ISC). 2017. On-line Event Bibliography. International Seismological Centre, Thatcham, UK. Available from http://www.isc.ac.uk/event_bibliography.

Kostrov, V.V. 1974. Seismic Moment and Energy of Earthquakes and Seismic Flow Of Rocks. Izv. Earth Physics, **1**: 23–40.

Kreemer, C., Blewitt, G., and Klein, E.C. 2014. A geodetic plate motion and Global Strain Rate Model. Geochemistry, Geophysics, Geosystems, **15**: 3849–3889. doi:10.1002/2014GC005407.

Kutu, J.M. 2013. Seismic and Tectonic Correspondence of Major Earthquake Regions in Southern Ghana with Mid-Atlantic Transform-Fracture Zones. International Journal of Geosciences, **4**: 1326–1332. doi:10.4236/ijg.2013.410128.

Kutu, J.M., Anani, C.Y., Asiedu, D.K., Manu, J., Hayford, E., and Oppong, I. . 2013. Recent Seismicity Of Southern Ghana And Re-Interpretation Of The 1939 Accra Earthquake: Implications for Major Recurrences Of Major Earthquakes. International Journal of Basic and Applied Sciences, **2**: 322–331. doi:10.14419/ijbas.v2i4.1120.

Langer, C.J., Bonilla, M.G., and Bollinger, G.A. 1987. Aftershocks and surface faulting associated with the intraplate Guinea, West Africa, earthquake of 22 December, 1983. Bulletin of the Seismology Society of America, **77**: 1579–1601.

Le, Pichon, X., and Hayes, D.E. 1971. Marginal Offsets, Fracture Zones, And The Early Opening Of The South Atlantic. Journal of Geophysical Research, **76**: 6283–6293. doi:10.1029/JB076i026p06283.

Lin, J., and Parmentier, E.M. 1989. Mechanisms of lithospheric extension at mid-ocean ridges. Geophysical Journal International, **96**: 1–22. doi:10.1111/j.1365-246X.1989.tb05246.x.

Mascle, J., and Blarez, E. 1987. Evidence for transform margin evolution from the Ivory Coast-Ghana continental margin. Nature, **326**: 378–381. doi:10.1038/326378a0.

Maus, S., Barckhausen, U., Berkenbosch, H., Bournas, N., Brozena, J., Childers, V., et al. 2009. EMAG2: A 2–arc min resolution Earth Magnetic Anomaly Grid Compiled From Satellite, Airborne, And Marine Magnetic Measurements. Geochemistry, Geophysics, Geosystems, **10**: 8. doi:10.1029/2009GC002471.

Meghraoui, M., Amponsah, P., Ayadi, A., Ayele, A., Ateba, B., Bensuleman, A.,

et al. 2016, The Seismotectonic Map of Africa. Episodes, **39**. doi:10.18814/epiiugs/2016/v39i1/89232.

Milesi, J.P., Frizon de Lamotte, D., de Kock, G., and Toteu, F. 2010. Tectonic Map of Africa, 2nd Edition. Commission for the Geological Map of the World.

Murray, J., and Segall, P. 2002. Testing Time-Predictable Earthquake recurrence by direct measurement of strain accumulation and release. Nature, **419**: 287–291. doi:10.1038/nature00984. PMID:12239564.

Mvondo Owono, F. 2010. Surrection cénozoïque de l'Ouest de l'Afrique à partir de deux exemples : le plateau sud-namibien et la marge nord camerounaise. Ph.D. dissertation, Université de Rennes (France).

Riboulot, V., Cattaneo, A., Berné, S., Schneider, R.R., Voisset, M., Imbert, P., and Grimaud, S. 2012. Geometry and chronology of late Quaternary depositional sequences in the Eastern Niger Submarine Delta. Marine Geology, **319–322**: 1–20. doi:10.1016/j.margeo.2012.03.002.

Rouland, D., Legrand, D., Cisternas, A., Streng, A., Gir, R., and Souriau, A. 2016, Historical seismicity in oceans from sailors' testimonies. Journal of Seismology, **20**: 251–264.

Sandwell, D.T., Müller, R.D., Smith, W.H.F., Garcia, E., and Francis, R. 2014. New Global Marine Gravity Model From CryoSat-2 and Jason-1 Reveals Buried Tectonic Structure. Science, **346**: 65–67. doi:10.1126/science.1258213. PMID: 25278606.

Scordilis, E.M. 2006. Empirical global relations converting *M*S and *m*b to moment magnitude. Journal of Seismology, **10**: 225–236. doi:10.1007/s10950-006-9012-4.

Smith, W.H.F., and Sandwell, D.T. 1997. Global Sea Floor Topography From Satellite Altimetry And Ship Depth Soundings. Science, **227**: 1956–1962. doi: 10.1126/science.277.5334.1956.

Weatherall, P., Marks, K.M., Jakobsson, M., Schmitt, T., Tani, S., Arndt, J.E., Rovere, M., Chayes, D., Ferrini, V., and Wigley, R. 2015. A new digital bathymetric model of the world's oceans. Earth and Space Science, **2**: 331–345. doi:10.1002/2015EA000107.

Wells, D.L., and Coppersmith, K.J. 1994. New empirical relationships among magnitude, rupture length, rupture width, rupture area, and surface displacement. Bulletin of the Seismology Society of America, **84**(4): 974–1002.

Wessel, P., and Smith, H.F. 1998. New, improved version of generic mapping tools released. Eos Transactions, AGU, **79**: 579. doi:10.1029/98EO00426.

Wilson, J.T. 1965. A new class of faults and their bearing on continental drift. Nature, **207**: 343–347. doi:10.1038/207343a0.

Wright, J.B. 1976. Fracture systems in Nigeria and initiation of fracture zones in the South Atlantic. Tectonophysics, **34**: 43–47.

NRC Research Press

CORRECTION

Correction: Active transform faults in the Gulf of Guinea: insights from geophysical data and implications for seismic hazard assessment

Mustapha Meghraoui, Paulina Amponsah, Paul Bernard, and Bekoa Ateba

Ref.: Can. J. Earth Sci. **56**(12): 1398–1408 (2019) dx.doi.org/10.1139/cjes-2018-0321.

On p. 1401, there were errors in eq. 4. The correct version is shown below:

$$\dot{M}_d = \mu \iint_S (\dot{U}_\alpha - \dot{U}) dS$$

Received 11 March 2020. Accepted 11 March 2020.

M. Meghraoui and P. Bernard. Institut de Physique du Globe de Strasbourg, CNRS–UMR 7516, France.
P. Amponsah. National Data Centre, National Nuclear Research Institute, Ghana Atomic Energy Commission, Accra, Ghana.
B. Ateba. Institute of Geological and Mining Research, Yaounde, and Mount Cameroon Volcano Observatory, Buea, Cameroon.
Corresponding author: Mustapha Meghraoui (email: m.meghraoui@unistra.fr).